Science of the Total Environment 953 (2024) 176225

Contents lists available at ScienceDirect

Science of the Total Environment

journal homepage: www.elsevier.com/locate/scitotenv

Assessing the size transformation of nanoplastics in natural water matrices

Aaron Boughbina-Portolés, Pilar Campíns-Falcó *

MINTOTA research group, Departament de Química Analítica, Facultat de Química, Universitat de València, Dr. Moliner 50, 46100 Burjassot, Valencia, Spain

HIGHLIGHTS

- Nanoplastics (NPs) were obtained from common plastic wastes by a nano-precipitacion method.
- Size stability of dispersions of PS, PET, PVC, PMMA and PC was assessed in different water matrices.
- None of the studied NPs was stable in seawater transforming into micro-plastics in less than a day.
- The order of aggregation in waters was: PET>PMMA>PVC > PC > PS in a period of 14 days.
- Size stability over time was worse for PS adding heteroaggregation and exposure to UV light.

GRAPHICAL ABSTRACT

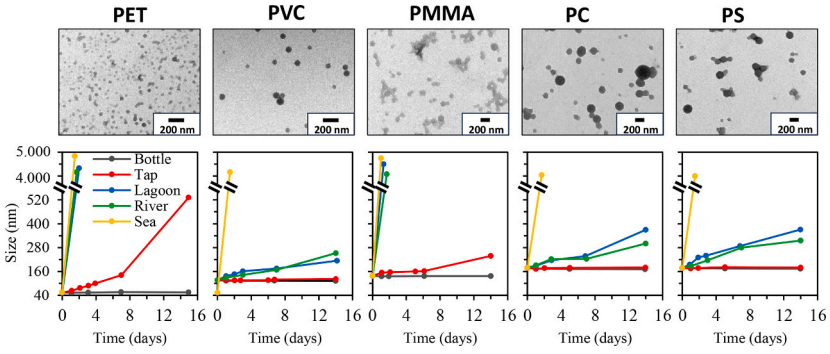

ARTICLE INFO

Editor: Damià Barceló

Keywords:
(Nano)plastics
Environmental waters
Stability
Size
Aggregation

ABSTRACT

Understanding the stability of NPs in different aqueous environments, related with their size is crucial for assessing their potential risks. This is influenced by several factors, including pH, ionic strength, and the presence of biomolecules, or dissolved organic matter (DOM). In this study, dispersions of NPs derived from common plastic waste materials, including polystyrene (PS), polyethylene terephthalate (PET), polyvinyl chloride (PVC), polymethyl methacrylate (PMMA), and polycarbonate (PC), were synthesized by a nanoprecipitation method with sizes: 189 ± 7, 58 ± 3, 123 ± 4, 151 ± 7 and 182 ± 6 nm, respectively. Stability for a period of 14 days of these NPs was assessed in various natural water matrices. Different analytical techniques were used, including Asymmetric Flow Field-Flow Fractionation (AF4) coupled with UV–Vis and Dynamic Light Scattering (DLS) in series, batch DLS, Fourier-Transform Infrared Spectroscopy-Attenuated Total Reflection (FTIR-ATR), and Transmission Electron Microscopy (TEM). None of the studied NPs was stable in seawater and NPs were transformed in microplastics (MPs) by aggregation. PET was more prone to aggregation in all waters and PS was the most stable followed for PC, PVC and PMMA. However, bottle and tap waters maintained better the original size of NPs. For the most stable dispersion PS, the influence of heteroaggregation in tap and lagoon waters and aging from exposure to UV light in sea water were tested. In both cases, the stability over time was worse for PS. The results can contribute to a more comprehensive understanding of the fate and behaviour of NPs in natural aquatic environments, emphasizing the importance of studying a wide range of polymers.

* Corresponding author.
E-mail address: pilar.campins@uv.es (P. Campíns-Falcó).

https://doi.org/10.1016/j.scitotenv.2024.176225
Received 7 July 2024; Received in revised form 21 August 2024; Accepted 10 September 2024
Available online 11 September 2024

1. Introduction

In recent decades, the widespread utilization of plastics due to their versatile range of applications has significantly driven global plastics production levels approached to 400 million metric tons by 2021 (Plastic production worldwide 2021). Consequently, because of inadequate waste management practices, plastic debris flow has emerged as a substantial pollutant in aquatic environments, where the presence of a wide array of plastics has already been reported (Ter Halle et al., 2017). Between them, polystyrene (PS from food packaging, insulation, consumer electronics), polyvinyl chloride (PVC from construction materials, pipes, flooring) and polyethylene terephthalate (PET from beverage bottles, food containers) stand out prevalent plastic polymers found in these environments. These plastics undergo weathering processes, including mechanical breakdown, biodegradation, and UV irradiation, predominantly, resulted in the formation of smaller particles known as microplastics (MPs) and nanoplastics (NPs) (El Hadri et al., 2020; Song et al., 2020; Wu et al., 2022).

There is a big concern regarding these particles, as the precise extent of their threat remains unknown, but there is consensus on the importance of studying them. In addition, NPs owing to their size, possess a large surface area, which results in an adsorption capacity that enables them to accumulate a variety of substances on their surface, such as organic pollutants or toxic trace metals (Massos and Turner, 2017; Alimi et al., 2018; Llorca et al., 2018). Furthermore, their small size makes them more likely to be ingested by aquatic fauna and incorporated into the food chain. It also allows NPs to easily penetrate cell barriers and get into circulatory system and tissues, causing cytotoxicity and behavioural disorders (Mattsson et al., 2017; Lehner et al., 2019; Cole et al., 2020; Shi et al., 2021). Nonetheless, the long-term effects are still poorly understood, although certain studies suggest a potential carcinogenic risk associated with NPs (Barguilla et al., 2022). Therefore, investigating the presence and, particularly, the transport and fate of NPs in natural aquatic environments is of vital importance.

As previously highlighted, the detrimental effects of NPs are primarily attributed to their small size, but size stability may depend on pH or ionic strength of the aqueous medium, as well as the presence of specific substances like biomolecules or dissolved organic matter (DOM) alongside other colloids such as clays (Sharma et al., 2021).

Thus, the hazardousness and persistence of NPs are strongly influenced by the aqueous medium in which they are found, as it can induce phenomena such as aggregation that can significantly alter their behaviour and characteristics. NPs stability primarily relies on their highly charged surface, which generates an electrostatic potential that constitutes an energetic barrier to the aggregation process. This potential promotes the formation of an ion-based electrical double layer. This double layer forms a protective shell around the NPs surface, effectively preventing their approach through electrostatic repulsion. However, numerous factors have the potential to screen this protective barrier in every water matrix as described by Boughbina-Portolés et al., 2021 for dispersions of Ag nanoparticles. Previous research for NPs has explored this subject, primarily focusing on a few types of polymers (predominantly PS and PMMA) (Ramirez et al., 2019; Wu et al., 2019) or utilizing dispersions of commercial NPs that exhibit substantial differences in terms of morphology, monodispersity, and surface chemistry compared to NPs found in real-world samples. Moreover, these dispersions often contain additives such as surfactants for stabilization and antimicrobial agents for preservation purposes. Thus, some studies have raised concern about the representativeness of NPs used in several studies to investigate their fate and behaviour, as well as their environmental and health hazard (Pikuda et al., 2019), and the need to study a broader range of polymers along with other factors like aging and weathering or heteroaggregation (Zhang et al., 2021).

Hence, the present study investigates by the first time the size transformation of NPs of PS, PET, PVC, Polymethyl methacrylate (PMMA) and Polycarbonate (PC) in natural aqueous matrices: bottled, tap, lagoon, river, transitional and sea. In addition, these NPs are obtained using the nanoprecipitation method from common plastic wastes to approximate to real situations, including packaging material, water bottles and pipes. In this method, the polymer of interest is solubilized in a solvent that is both able to dissolve it and miscible with water, while also having a lower boiling point. The resulting solution is slowly poured into ultrapure water while maintaining constant and vigorous stirring, leading to saturation of polymer macromolecules. This process triggers the nucleation and subsequent growth of the NPs (Wang et al., 2016; Zielinska et al., 2020). The size changes in the several water matrices were evaluated here by using several techniques: asymmetrical flow field-flow fractionation (AF4) with UV–vis and dynamic light scattering (DLS) detectors in series, batch DLS and transmission electron microscopy (TEM). Fourier-transform infrared spectroscopy-attenuated total reflection (FTIR-ATR) was employed with identification purposes. Heteroaggregation and aging by exposure to UV-light were also studied.

2. Experimental

2.1. Reagents and materials

Commercial solutions of 10 % (*w/v*) PS latex beads (100, 300 and 600 nm mean particle size) containing 0.1 % sodium azide were obtained from Sigma-Aldrich (St. Louis, MO, USA). Hexafluoroisopropanol (HFIP) $\geq$ 99 % was also supplied by Sigma-Aldrich, and tetrahydrofuran (THF) GPC grade ACS stabilized with 250 ppm of 2,6-Di-tert-butyl-4-methylphenol (BHT) was purchased from Scharlab (Barcelona, Spain). Plastic materials for preparing nanoparticles were obtained from common waste, such as packaging material, water bottles and pipes, and identified by means of FTIR-ATR.

AF4 with detectors UV–vis and DLS in series works with a liquid carrier (0.1 μm filtered) prepared with 0.01 % sodium dodecyl sulfate (SDS) from Panreac (Barcelona, Spain). A Water:Methanol (VWR, Radnor, PA, USA) 80:20 ratio mixture was used for cleaning the AF4 system. Ultrapure water for all the experiments was purified using a B-30 Bio system from Adrona (Riga, Latvia) (ρ = 18.2 MΩ·cm; Total organic carbon <2 ppb).

2.2. Instrumentation

The AF4 system used was an AF2000 MultiFlow FFF from Postnova Analytics Inc. (Landsberg am Lech, Germany) coupled on-line to the UV–Vis detector SPD-20AV (Shimadzu Corporation, Kyoto, Japan) and the DLS detector Zetasizer Nano ZS (Malvern, UK). Flows were provided by two separate PN1130 isocratic pumps from Postnova Analytics Inc. equipped with the PN7520 degasser, and the cross-flow was obtained by a separate piston pump, which is constantly adjustable. DLS detector can work in batch mode too. Table S1 of the supporting information (SI) summarizes the optimal conditions for batch DLS measurements.

FTIR-ATR spectra were measured with the Cary 630 FTIR spectrometer from Agilent (Santa Clara, CA, USA), by drying a 5 μL drop on the ATR crystal and measuring the spectrum of the solid. A electron microscopy JEM 1010 from JEOL Ltd. (Tokyo, Japan) operated at 80 kV was employed. Transmission electron microscope (TEM) samples were prepared by delivering 2.5 μL of the aqueous NP dispersion onto a carbon-coated copper grid (300 mesh) and were dried overnight at room temperature.

Additionally, natural water samples of the Valencian Community (Spain) were characterized potentiometrically using ion-selective electrodes (ISEs) provided by ThermoFisher (Waltham, MA, USA) for sodium and chloride, and one from Metrohm (Herisau, Switzerland) for calcium.

An ICT Beam Boost photochemical reaction unit from Austria equipped with a UV lamp (254 nm, 8 W) was also employed.

2.3. Preparation of NPs

NPs dispersions were prepared by adding 2 mg of PS, PVC, PMMA or PC waste to 1 mL of THF, or 2 mg of PET to 1 mL of HFIP until completely dissolved. Subsequently, 0.5 mL of the dissolved polymer solutions were slowly added (at a rate of approximately 0.5 mL·min^{-1}) with a Hamilton syringe into a vial containing 10 mL of ultrapure water under constant magnetic stirring at 600 rpm. The water in the vials immediately turned cloudy, indicating the formation of the NPs dispersion. Stirring was maintained for a further 15 min to ensure that the process is completed. The resulting suspensions were kept at 90 °C until its volume is reduced to 1 mL in order to concentrate NPs, while evaporating any traces of organic solvent that may remain, and then they were filtered through a 1 μm pore size glass fibre filter. After NPs dispersions were obtained, NPs concentration was determined gravimetrically and characterized by DLS, AF4-UV-DLS, FTIR-ATR and TEM in order to determine their size distribution, polydispersity, composition, surface charge and morphology.

2.4. Stability of NPs in different aqueous matrices

To assess the stability of the different NPs in various aqueous matrices, samples of bottled (BW), tap (TW), lagoon (LW), river (RW), transitional (TW) and sea (SW) waters were employed. All aqueous matrices were filtered using a 0.1 μm pore size polysulfone (PES) filter to eliminate potential nanosized interferents. The NPs solutions were diluted at a 1:10 ratio with each water sample to minimize matrix alterations. Subsequently, the diluted solutions were stored, and their measurements were recorded over a 14-day period. AF4-UV-DLS and batch mode DLS techniques were employed to monitor the evolution of the NPs.

2.5. Heteroaggregation

To study the heteroaggregation process, a dispersion of PET and PS NPs was prepared and diluted at a 1:10 ratio in each of the aqueous matrices. They were then stored for 24 h, and their evolution was assessed using AF4-UV-DLS in order to compare it with the individual dispersions of each plastic.

2.6. Aging by exposure to UV light

A photochemical reaction unit equipped with a UV lamp (254 nm, 8 W) was employed to investigate the impact of aging on the PS NPs. PS NPs dispersions were placed in glass petri dishes under the UV lamp with occasional manual shaking to prevent potential sedimentation of the NPs. Then, the resulting dispersions were filtered using a 1 μm pore size glass fibre filter, and measured by DLS, AF4-UV-DLS and FTIR in order to compare the results with the unaged dispersions. Also, solid shredded expanded PS waste was exposed to UV lamp and analysed by FTIR to observe the chemical transformations that take place during PS aging.

3. Results and discussion

3.1. Characterization of synthetized NPs dispersions

The dispersions of the five synthetized NPs in ultrapure water (see Section 2.3) were characterized using DLS batch mode (Table 1 and Fig. 1a), FTIR-ATR (Fig. 2) and TEM (Fig. 3). NPs exhibit different size distributions depending on the polymer type for PS, PVC, PMMA and PC soluble in THF and PET soluble in HFIP as Fig. 1a shows. PET dispersion presented the smallest NP size as Table 1 indicated. NP dispersions show a low polydispersity index (PDI < 0.1) by batch DLS and a highly negative surface charge as deduced from zeta potential data, which gives them great stability (Table 1). Zeta potential data given in Table 1 are consistent with those obtained in NPs produced by methods distinct from the one used in this study, such as mechanical fragmentation (Ekvall et al., 2019; El Hadri et al., 2020).

Table 1
Average hydrodynamic diameter (batch DLS and AF4-DLS), polydispersity index (PDI) and zeta potential (ZP) for all obtained NPs dispersions in ultrapure water for $n = 5$.

Plastic	Batch DLS size (nm)	AF4-DLS size (nm)	PDI	Zeta Potential (mV)
PET	53 ± 1	58 ± 3	0.075	-30 ± 2
PS	177 ± 2	189 ± 7	0.093	-38 ± 1
PVC	116 ± 2	123 ± 4	0.059	-38 ± 3
PMMA	138 ± 1	151 ± 7	0.067	-38 ± 2
PC	180 ± 1	182 ± 6	0.060	-42 ± 1

As it can be seen in Fig. 2, FTIR analysis confirms that the composition of the NPs matches that of the starting material, as evidenced by the coincidence of characteristic peaks. In addition, Fig. 3 displays TEM images of the dispersions of the five NPs produced, showcasing their core size and morphology. As it can be observed, all the produced NPs exhibit a spherical morphology. Also, TEM images reveal the absence of porosity or multilayer structures in the NPs, indicating their solid and compact nature. Fig. 3 shows that the smallest particles corresponded to the PET dispersions in accordance with that obtained by batch DLS, which gives hydrodynamic diameter instead of core size as TEM. Monodispersity is also showed in Fig. 3.

3.2. Size assessment of NP dispersions by AF4

A separation technique as AF4 is needed to corroborate size assessment of the synthetized NPs dispersions. In order to achieve effective size-dependent separation, key parameters including the choice of carrier liquid, membrane type, and, most importantly, cross-flow (C_F) profile, were optimized. These variables are given in Table 2 to provide detailed insights into the experimental setup and optimization process.

A SDS solution was selected as the carrier liquid because it is an anionic surfactant that coats the NPs, imparting a more negative surface charge and enhancing their stability in the AF4 run (see Table S2 in SI). Furthermore, the membrane of the AF4 system utilized under the given conditions carries a positive charge, leading to increased electrostatic repulsion with the NPs. This phenomenon contributes to peak narrowing and reduced retention times, while also enhancing sensitivity in front of other possible carrier like NaN_3 as it can be seen in Fig. S1 in SI. Durability of the membrane by minimizing NPs adhesion to its surface is also improved.

On the other hand, a C_F profile was selected with a high flow rate at the beginning to reduce the size of the void peak, followed by an exponential gradient to zero to ensure elution of all sample components. With all these parameters optimized, the five NP dispersions were assayed (Fig. 1b). The fractograms obtained by using UV–Vis detection at 240 nm indicate that only a population of NP is obtained, confirming the monodispersity of the different NP dispersions. Fig. 1b also includes the measured size by the DLS detector in series with UV–Vis detector and Fig. 1c indicates the structure of the five polymers. The sizes obtained by AF4-DLS were similar to those provides by batch DLS as Table 1 shows. A t paired test ($t = -3.744$, p value $= 0.02$) indicated at a confidence interval of 98 % that the results obtained by the two techniques are statistically similar and also the regression model obtained, which was (y = x): $y = (-4 \pm 7) + (0.98 \pm 0.05)x$ and $R^2 = 0.993$, being y and x the mean values obtained by batch DLS and by AF4-DLS (see Table 1), respectively. A dispersion of standard PS nanobeads with three different sizes (100, 300, and 600 nm) was utilized to evaluate the separation performance of the method. The corresponding results are illustrated in Fig. 4.

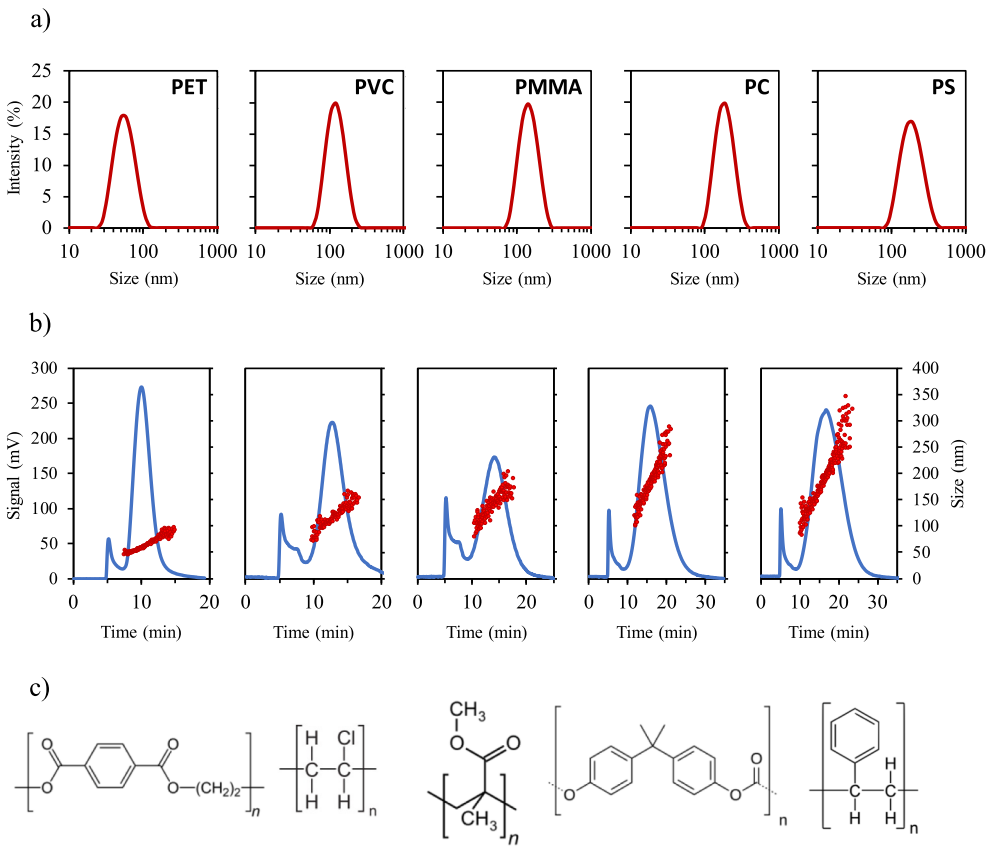

Fig. 1. (a) Batch mode DLS records, (b) fractograms UV–Vis including on line values of size obtained by DLS for dispersions of all produced NPs: PET 30 mg/L; PVC 84 mg/L; PMMA 75 mg/L; PC 15 mg/L; PS 15 mg/L and (c) structure of the studied polymers.

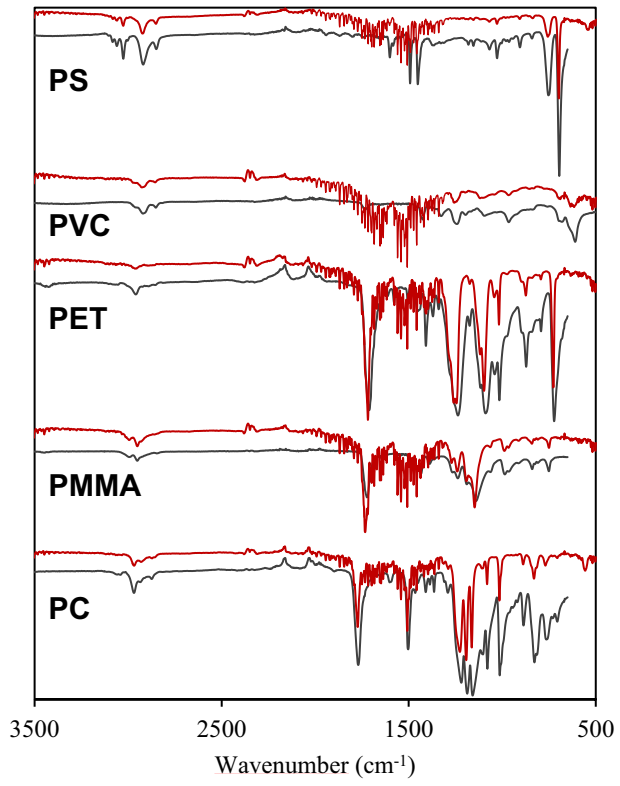

Fig. 2. IR spectra of the starting material (black line) and the corresponding nanoparticles (red line) for the five plastics investigated.

3.3. Stability over time of NPs in different aqueous matrices

The previously optimized experimental conditions of AF4 were utilized to assess the stability over time of the NPs in various aqueous matrices listed in Table 3. Some physical chemical parameters were measured: pH, conductivity, and the concentration of sodium, chloride and calcium and values between 6.93 and 8.39, 54–48,560 $\mu S \cdot cm^{-1}$, 1.2–14,050 mg/L, 47–25,110 mg/L and 6.5–389 mg/L, respectively, were obtained.

Fig. 5 displays the stability study data obtained by means of AF4-UV-DLS and batch DLS, revealing significant variations among the different types of NPs as well as across the diverse aqueous matrices studied.

As it can be observed, there is a clear correlation between the ionic strength of the medium (see Table 3) and the low stability of the NPs shown in Fig. 5. This can be attributed to the electro-stabilization mechanism of the NPs arising from their high surface charge (as evident from the zeta potential data). The presence of a high concentration of ions screens this electric potential, thereby reducing the repulsion between NPs and making their aggregation into larger NPs or Micro (MPs) more energetically favourable. This mentioned behaviour for NPs are similar to those provided by other types of nanosized materials, like silver (Baalousha et al., 2013; Boughbina-Portolés et al., 2021) and metal oxide (Keller et al., 2010).

Certain characteristics of natural waters, such as the presence of DOM, can provide steric stabilization to nanosized materials (Baalousha et al., 2013) and may contribute to the stability of NPs. However, it is evident that none of the studied NPs are stable in seawater as it can be seen in Fig. 5 and the influence of DOM was negligible. The peaks of the fractograms given in Fig. 1b disappear in a day and the % relative areas corresponding to all NPs is 0 as Fig. 5 indicates. Sizes given by batch DLS indicate that MPs were obtained.

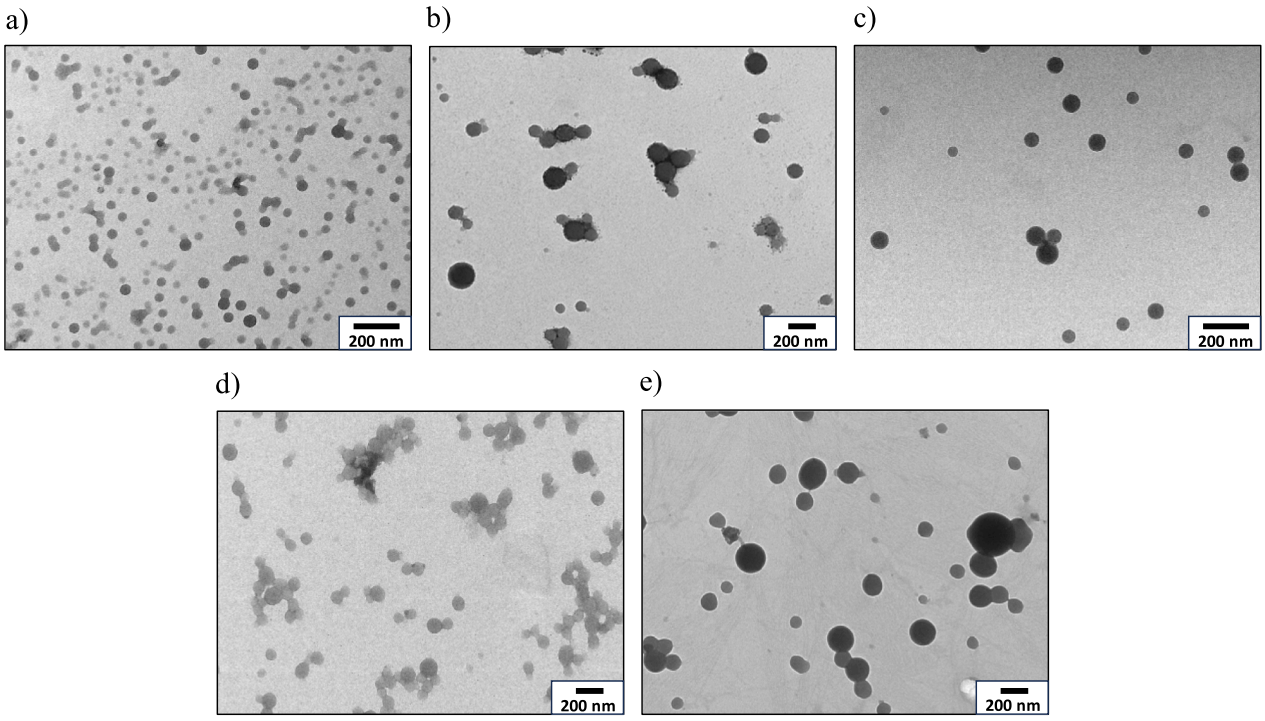

Fig. 3. Micrographs obtained for dispersions of (a) PET, (b) PS, (c) PVC, (d) PMMA and (e) PC NPs by means of TEM. Scale bar 200 nm.

Table 2
Optimal instrumental variables and conditions of the AF4 system for the separation of NPs.

Channel parameters	Length	Long channel (290 mm)		
	Spacer	350 μm thick		
Membrane	Type	Regenerated cellulose		
	MWCO	5 kDa		
Carrier liquid		SDS 0.01 % (*w/v*)		
Flows	Injection Flow (I_F)	0.20 mL·min^{-1}		
	Detector Flow	0.50 mL·min^{-1}		
	Initial Cross Flow (C_F)	2.0 mL·min^{-1}		
Times	Focus Time (F_T)	4.0 min.		
Injection	Type	Manual		
	Volume	100 μL		
Detectors		DLS and UV–Vis (240 nm)		
Sequence	Mode	Length (min.)	C_F (mL·min^{-1})	Gradient
	(1) Injection + Focus	4.0	2.0	–
	(2) Transition	0.5	2.0	–
	(3) Elution	2.5	2.0	–
	(4) Elution	0.25	2.0 to 1.0	Linear
	(5) Elution	23.0	1.0 to 0.25	Exp. (0.25)
	(6) Elution	7.5	0.25 to 0.0	Linear
	(8) Elution	10	0	–

On the other hand, in the case of less saline waters, the NPs exhibit a certain level of stability for several days, which depends on the type of water and, more importantly, the type of NPs. Specifically, PET NPs presented more aggregation, as they exhibit only partial stability in very low ionic strength media, such as bottled water (see Fig. 5 a). This can be attributed to their relatively less negative zeta potential and smaller size (Table 1), which results in higher surface energy and promotes the irreversible aggregation process.

For the remaining NPs, all exhibit high stability in low-saline media such as bottled or tap water, maintaining approximately 80 % and

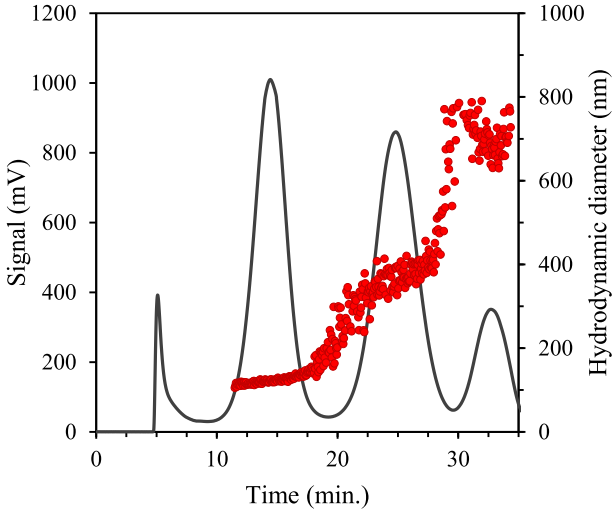

Fig. 4. Fractogram of a dispersion containing standard PS nanobeads with three different sizes (100, 300, and 600 nm) obtained using the optimized conditions of the AF4-UV-DLS system.

Table 3
Values of pH, conductivity, and concentration values (in mg/L) of some ions in the samples of natural aqueous matrices used to evaluate the stability over time of the NPs dispersions.

Water	pH	Conductivity (μS·cm^{-1})	[Na^+]	[Cl^-]	[Ca^{2+}]
Bottle	6.93	54	1.2	47	6.5
Tap	8.15	1110	139	206	109
Lagoon	8.39	1764	109	673	389
River	7.99	1560	78	258	263
Sea	8.07	48,560	14,050	25,110	228
Transition	7.47	12,060	2113	6652	192

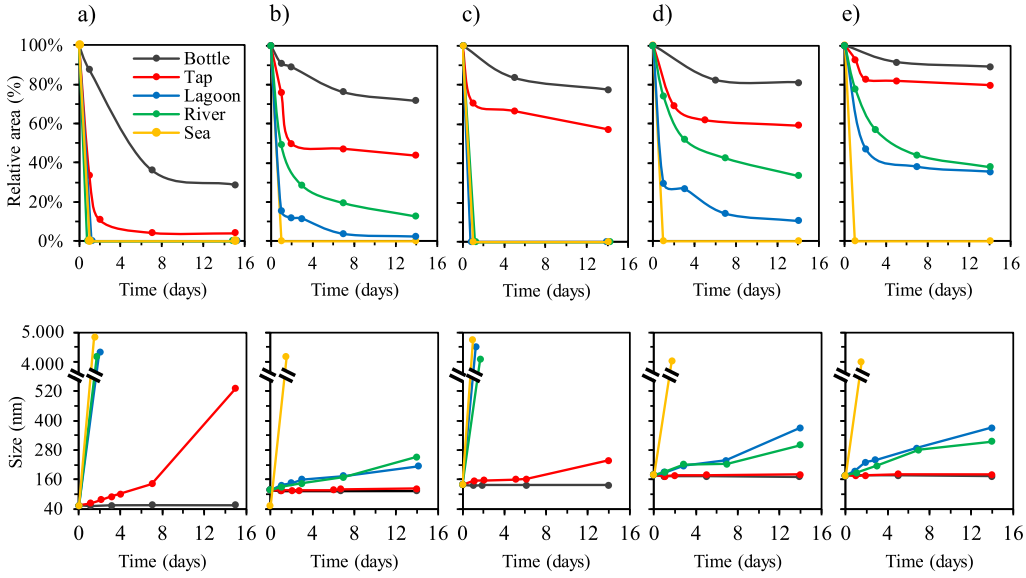

Fig. 5. Evolution of relative area of fractogram peaks obtained by AF4-UV-DLS and average size of the dispersions measured by batch DLS for (a) PET, (b) PVC, (c) PMMA, (d) PC, and (e) PS NPs dispersions in different aqueous matrix samples over a 14-day period.

60–70 % of the peak area, respectively, after 14 days. In higher ionic strength water, as anticipated, a greater degree of aggregation is observed. However, the PC and PS NPs display remarkable persistence, with PS demonstrating the highest stability among the NPs investigated, maintaining around 50 % of the peak area in lagoon and river after the 14-day period. As indicated before, in seawater PS also shows aggregation and this is corroborated by results in Fig. 6, which gives TEM images (a and b) of the aggregates and the fractogram obtained (c) without the peak corresponding to NPs. All NPs maintain their size practically unchanged in bottled water and also in tap water, except for PET and PMMA NPs, which undergo minor aggregation but remain at the nanometre scale (531 nm and 238 nm, respectively, after 14 days). Fig. 7 indicates that the process related with the increment of the size of the dispersions is aggregation and no agglomeration because sonication of NPs did not permit to obtain the original size dispersion. Fig. 7 shows the results obtained for PET and PS NPs dispersions in river and sea water, respectively, as an example.

On the other hand, in lagoon and river, PET and PMMA NPs experience rapid aggregation, similar to that observed in seawater. However, the remaining NPs exhibit a certain level of stability, with their average size doubling over a 14-day period, while still remaining within the nanometre range.

This type of behaviour, where two very different aggregation regimes are observed depending on the ionic strength of the medium, is

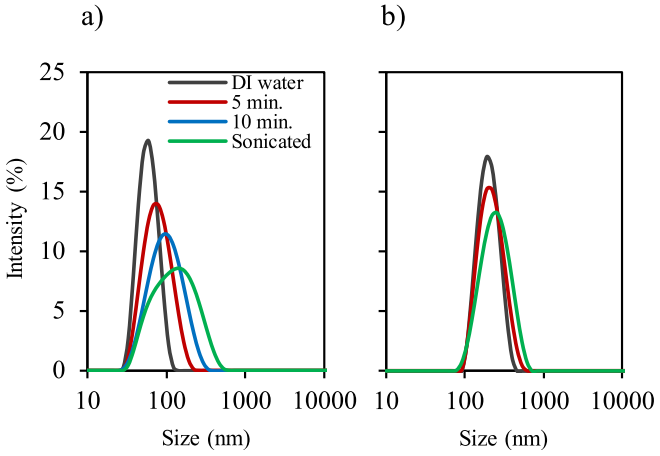

Fig. 7. Batch mode DLS records of the time evolution of PET and PS NPs dispersions in river and sea water respectively, and ultrasonicated dispersions.

characteristic of the DLVO theory (Li et al., 2018; Liu et al., 2019), which states that the stability of a colloidal dispersion is determined by the interplay of two opposite forces: electrostatic repulsion, resulting from

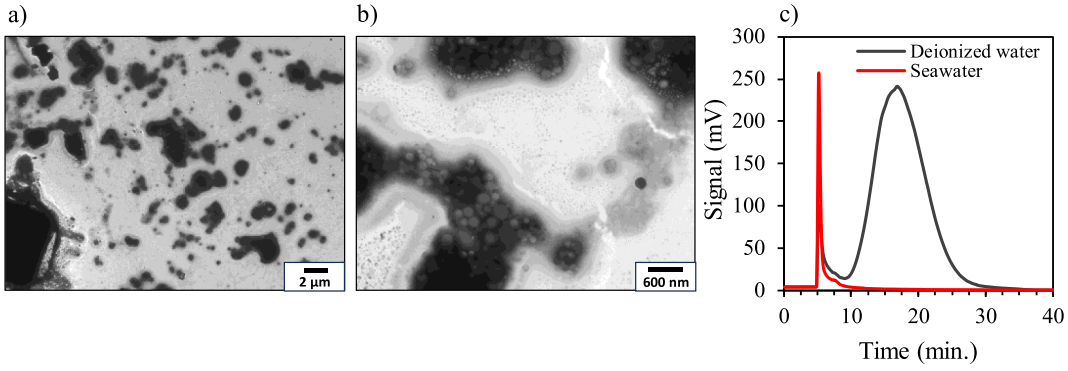

Fig. 6. Micrographs obtained for a PS NPs dispersion in seawater after a 14-day period by means of TEM. Scale bar (a) 2 µm and (b) 600 nm. (c) Fractogram comparison for PS NPs in seawater after 14 days and in deionised water.

the surface charge of the particles, and Van der Waals forces of attraction, so the resulting force determines the stability of the colloid. When the repulsive force outweighs the attractive force, aggregation occurs at a slow rate, known as the reaction-limited aggregation regime. In this regime, the NPs are partially stabilized by the electrostatic repulsion between particles, as most likely observed for PS NPs. Conversely, when the attractive force is dominant, aggregation proceeds through fast kinetics, a situation known as diffusion-controlled aggregation regime. This regime occurs when the charge surrounding the NPs is sufficiently screened, reducing the energy barrier to aggregation, as seen in the case of PET NPs. The transition point between the two situations is known as the critical coagulation concentration (CCC) (Hsu and Liu, 1998; Hiemenz and Rajagopalan, 2016), so that if the ionic strength of the medium is below this value, the dispersion should remain at least partially stable. However, if the ionic strength exceeds the CCC, a rapid aggregation process is expected to occur, so this value can therefore also be understood as an indicator of colloidal stability.

With all the aforementioned data, it can be inferred that there are notable variations in the stability of the nanoparticles (NPs) depending on the polymer, as a higher stability is observed in the following order: PET < PMMA < PVC < PC < PS. Moreover, the presence of NPs is anticipated to present a substantial risk in drinking water and low-salinity natural waters, such as river water or similar environments, warranting careful attention. However, the occurrence of NPs in seawater is unlikely, thereby minimizing the potential for significant risks in such settings.

3.4. Heteroaggregation and aging from UV light of PS-NPs

For the most stable nanoplastic PS over time in the different environmental waters, other variables in addition to water composition were tested as heteroaggregation and aging by exposure to UV light. Fig. 8 presents a comparison of the aggregation process of PS and PET NPs when they are dispersed individually and together.

As observed, the stability of both NPs is considerably diminished when they are together since the aggregation rate increases. For PS NPs, the aggregation rate rises by over 300 % in tap water and slightly below 30 % in lagoon water, whereas PET NPs experience an increase of nearly 40 %. These findings clearly indicate that the presence of other colloids significantly reduces the stability of the NPs. Similar effects have been observed in the presence of clays and other inorganic colloids (Singh et al., 2019). Thus, the issue of NPs becomes more delicate, as they may not only exist in isolation but also form part of other structures and associate with other colloidal substances.

Finally, it is crucial to consider that plastic waste in real-life conditions is often exposed to UV light. These external factors can induce changes that alter its properties compared to pristine plastic. These changes can also alter the properties and characteristics of the NPs derived from them, thus impacting their stability.

Fig. 9 shows the evolution of the IR spectrum of a pristine sample of PS waste under prolonged exposure to UV light. The spectrum exhibits a gradual increase in a peak located around 1720 cm^{-1}, which corresponds to the carbonyl group that develops when oxygen is incorporated into the polymer structure during the photooxidation process. This can be confirmed by calculating the carbonyl index for each spectrum (Pristine: 0.03; 6 h: 0.21; 24 h: 0.36; 48 h: 0.71; 120 h: 1.04), as it provides a value that quantifies the ratio of carbonyl groups present in the sample (Rodrigues et al., 2018; Mao et al., 2020), and is calculated as follows:

$$I_C = \frac{A_{C=O}}{A_C} \quad (1)$$

where $A_{C=O}$ is the absorbance at carbonyl peak (1720 cm^{-1}), and A_C is the absorbance of the peak located at 1450 cm^{-1}. Furthermore, the spectra show a slight increase above 3100 cm^{-1}, which corresponds to the characteristic peak of hydroxyl group that is likewise integrated into the polymer structure (Cai et al., 2018).

This occurs in a similar way in the case of PS NPs dispersions, as deduced from the carbonyl index values provided in Table 4. Also, a clear reduction of the average size can be observed with increasing irradiation time, while no significant changes in the zeta potential are detected.

The reduction in particle size can be attributed to the impact of UV light exposure on plastics. Several studies on microplastics have demonstrated that exposure to UV light induces surface cracking and the generation of smaller plastic fragments (Song et al., 2017; Wang et al., 2020). Also, this phenomenon may be related to alterations in the surface structure of the NPs, potentially caused by chain breakage resulting from the impact of free radicals, including peroxyl (ROO·), alkoxyl (RO·), and hydroxyl (·OH) radicals (Bracco et al., 2018). Additionally, extensive research has implicated UV light aging as a significant contributor to the release of NPs into the environment. Researchers have observed the formation of NPs from various materials originating from sources such as microplastics, conventional bags, masks, among others (Song et al., 2017; Wang et al., 2020; Tong et al., 2022; Liang et al., 2023; Wu et al., 2023).

In terms of colloidal stability, the zeta potential data for these

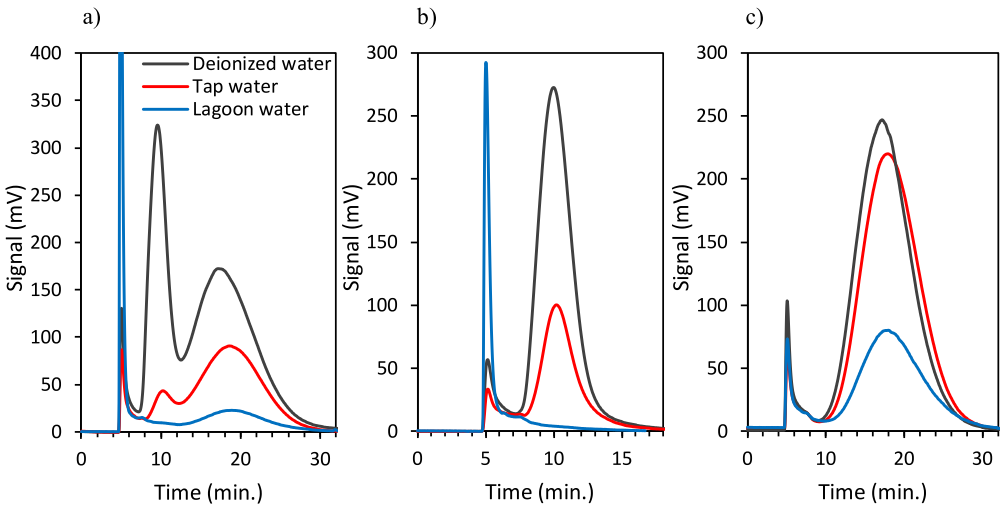

Fig. 8. Fractograms of (a) a PS and PET dispersion, (b) an isolated PET dispersion, and (c) an isolated PS dispersion obtained by AF4-UV in different aqueous matrices after 24 h.

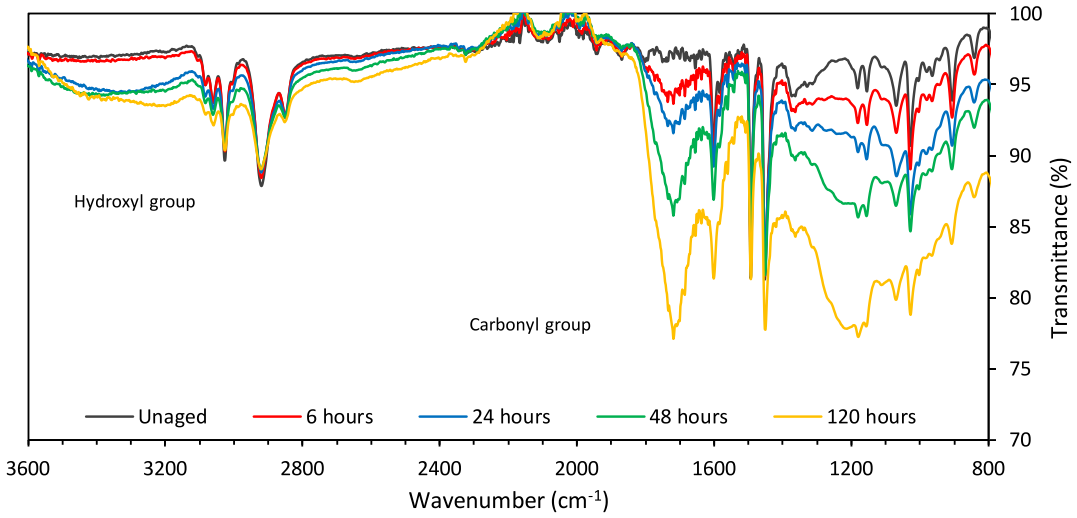

Fig. 9. IR spectra evolution of a pristine sample of PS waste under prolonged exposure to UV light.

Table 4
Average size and zeta potential values for PS NPs dispersions from batch DLS aged for different periods of time by exposure to UV irradiation for n = 5.

Aging time (h)	Carbonyl index	Average size (nm)	Zeta Potential (mV)
Unaged	0.03	189.6 ± 0.4	−36.0 ± 0.5
2	0.69	184.4 ± 0.2	−35.1 ± 0.3
4	0.79	182.1 ± 1.1	−35.0 ± 0.5
6	1.08	175.3 ± 1.2	−35.5 ± 0.1

dispersions is presented in Table 4. It can be observed that there is no apparent change in the zeta potential with aging, as it remains similar to that of the unaged plastic. However, as depicted in Fig. 10, a notable difference in stability is observed in seawater, where pristine NPs exhibited greater resistance to aggregation. Generally, it has been proposed that aging NPs should enhance their stability by increasing their polarity, thereby reducing their hydrophobicity due to the decrease of van der Waals attraction forces and the increase of electrical double-layer repulsion from O-containing functional groups undergoing deprotonation (Liu et al., 2019; Mao et al., 2020). Nevertheless, this trend is only observed in seawater, as no significant difference in stability is observed in the other aqueous matrices.

4. Conclusions

A study has been conducted to assess the stability of various NPs made from different materials in different natural aqueous matrices. For this study, NPs dispersions were obtained through the nanoprecipitation method from various types of plastic waste to approximate to real-world samples. Furthermore, the AF4-UV-DLS technique has been shown to be a very robust alternative for the qualitative and quantitative analysis of NPs, as it is able to perform size separation of nanosized materials without the need for interaction with a stationary phase.

With regard to the stability of the NPs studied, they have generally shown in aqueous matrices except for seawater the conservation at the nanometric scale (< 400 nm) for more than two weeks thanks to their high surface charge. Generally, aggregation of the initial NPs was observed. However, in high salinity environments such as seawater, this protection is greatly reduced, making it very unlikely to find NPs in dispersion, as they are able to transform into microplastics (> 4 μm) in less than a day. It has also been observed for the most stable NP like PS that the presence of other NP as PET reduces its stability by introducing the mechanism of heteroaggregation, increasing the rate of aggregation by >300 % in tap water, and by 30–40 % in lagoon water. The aging of

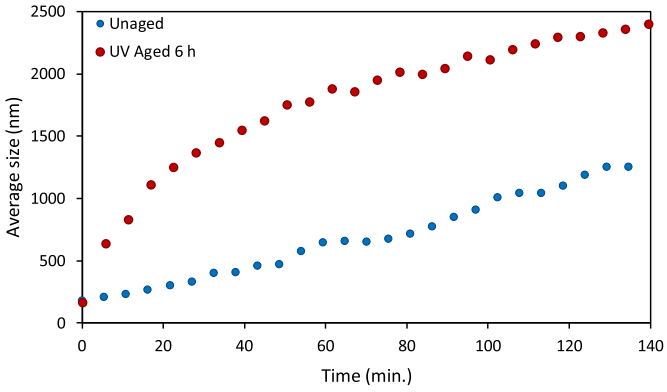

Fig. 10. Evolution of the mean size of pristine and aged PS NPs over time in seawater.

PS NPs has also been studied, where the incorporation of oxygen into the polymer structure has been observed. Aging increased the aggregation rate of PS NPs in seawater, but this trend does not occur in the other aqueous matrices studied.

This paper is intended to contribute to know the real extent of the NPs problem as a potential danger to fauna and flora, as well as a possible risk to human health.

CRediT authorship contribution statement

Aaron Boughbina-Portolés: Writing – original draft, Validation, Methodology, Investigation. **Pilar Campíns-Falcó:** Writing – review & editing, Writing – original draft, Supervision, Resources, Project administration, Methodology, Investigation, Funding acquisition, Conceptualization.

Declaration of competing interest

The authors declare that they have no known competing financial interests or personal relationships that could have appeared to influence the work reported in this paper.

Data availability

Data will be made available on request.

Acknowledgements

This work was supported by Projects: PID2021-124554NB-I00 funded by MCIN/AEI/10.13039/501100011033 and by "ERDF A way of making Europe" by the European Union; PROMETEO Program 2020/078 funded by Generalitat Valenciana (Conselleria de Educación, Cultura, Universidades y Empleo) and ID-FEDER/2018/ 049 funded by Generalitat Valenciana and "ERDF A way of making Europe" by the European Union. A.B.-P. expresses his gratitude to the Generalitat Valenciana for the grant (CIACIF/2021/069).

Appendix A. Supplementary data

Supplementary data to this article can be found online at https://doi.org/10.1016/j.scitotenv.2024.176225.

References

Alimi, O.S., Farner Budarz, J., Hernandez, L.M., Tufenkji, N., 2018. Microplastics and nanoplastics in aquatic environments: aggregation, deposition, and enhanced contaminant transport. Environ. Sci. Technol. 52, 1704–1724. https://doi.org/10.1021/acs.est.7b05559.

Baalousha, M., Nur, Y., Römer, I., Tejamaya, M., Lead, J.R., 2013. Effect of monovalent and divalent cations, anions and fulvic acid on aggregation of citrate-coated silver nanoparticles. Sci. Total Environ. 454–455, 119–131. https://doi.org/10.1016/J.SCITOTENV.2013.02.093.

Barguilla, I., Domenech, J., Ballesteros, S., Rubio, L., Marcos, R., Hernández, A., 2022. Long-term exposure to nanoplastics alters molecular and functional traits related to the carcinogenic process. J. Hazard. Mater. 438, 129470 https://doi.org/10.1016/J.JHAZMAT.2022.129470.

Boughbina-Portolés, A., Sanjuan-Navarro, L., Moliner-Martínez, Y., Campíns-Falcó, P., 2021. Study of the stability of citrate capped Agnps in several environmental water matrices by asymmetrical flow field flow fractionation. Nanomaterials 11, 926. https://doi.org/10.3390/nano11040926.

Bracco, P., Costa, L., Luda, M.P., Billingham, N., 2018. A review of experimental studies of the role of free-radicals in polyethylene oxidation. Polym. Degrad. Stab. 155, 67–83. https://doi.org/10.1016/J.POLYMDEGRADSTAB. 2018.07.011.

Cai, L., Wang, J., Peng, J., Wu, Z., Tan, X., 2018. Observation of the degradation of three types of plastic pellets exposed to UV irradiation in three different environments. Sci. Total Environ. 628–629, 740–747. https://doi.org/10.1016/J.SCITOTENV.2018.02.079.

Cole, M., Liddle, C., Consolandi, G., Drago, C., Hird, C., Lindeque, P.K., Galloway, T.S., 2020. Microplastics, microfibres and nanoplastics cause variable sub-lethal responses in mussels (Mytilus Spp.). Mar. Pollut. Bull. 160, 111552 https://doi.org/10.1016/J.MARPOLBUL.2020.111552.

Ekvall, M.T., Lundqvist, M., Kelpsiene, E., Šileikis, E., Gunnarsson, S.B., Cedervall, T., 2019. Nanoplastics formed during the mechanical breakdown of daily-use polystyrene products. Nanoscale Adv. 1, 1055–1061. https://doi.org/10.1039/C8NA00210J.

El Hadri, H., Gigault, J., Maxit, B., Grassl, B., Reynaud, S., 2020. Nanoplastic from mechanically degraded primary and secondary microplastics for environmental assessments. NanoImpact 17, 100206. https://doi.org/10.1016/J.IMPACT.2019.100206.

Hiemenz, P.C., Rajagopalan, R., 2016. Principles of colloid and surface chemistry: third edition, revised and expanded. Princ. Colloid Surf. Chem. Third Ed. Revis. Expand. 1–650. https://doi.org/10.1201/9781315274287/PRINCIPLES-COLLOID-SURFACE-CHEMISTRY-REVISED-EXPANDED-PAUL-HIEMENZ-RAJ-RAJAGOPALAN.

Hsu, J.P., Liu, B.T., 1998. Effect of particle size on critical coagulation concentration. J. Colloid Interface Sci. 198, 186–189. https://doi.org/10.1006/JCIS.1997.5275.

Keller, A.A., Wang, H., Zhou, D., Lenihan, H.S., Cherr, G., Cardinale, B.J., Miller, R., Zhaoxia, J.I., 2010. Stability and aggregation of metal oxide nanoparticles in natural aqueous matrices. Environ. Sci. Technol. 44, 1962–1967. https://doi.org/10.1021/es902987d.

Lehner, R., Weder, C., Petri-Fink, A., Rothen-Rutishauser, B., 2019. Emergence of nanoplastic in the environment and possible impact on human health. Environ. Sci. Technol. 53, 1748–1765. https://doi.org/10.1021/acs.est.8b05512.

Li, S., Liu, H., Gao, R., Abdurahman, A., Dai, J., Zeng, F., 2018. Aggregation kinetics of microplastics in aquatic environment: complex roles of electrolytes, PH, and natural organic matter. Environ. Pollut. 237, 126–132. https://doi.org/10.1016/J.ENVPOL.2018.02.042.

Liang, H., Guo, R., Liu, D., Song, N., Wang, F., Li, Y., Ge, W., Chai, C., 2023. The behavior of microplastics and nanoplastics release from UV-aged masks in the water. Sci. Total Environ. 891, 164361 https://doi.org/10.1016/J.SCITOTENV.2023.164361.

Liu, Y., Hu, Y., Yang, C., Chen, C., Huang, W., Dang, Z., 2019. Aggregation kinetics of UV irradiated nanoplastics in aquatic environments. Water Res. 163, 114870 https://doi.org/10.1016/J.WATRES.2019.114870.

Llorca, M., Schirinzi, G., Martínez, M., Barceló, D., Farré, M., 2018. Adsorption of perfluoroalkyl substances on microplastics under environmental conditions. Environ. Pollut. 235, 680–691. https://doi.org/10.1016/J.ENVPOL.2017.12.075.

Mao, Y., Li, H., Huangfu, X., Liu, Y., He, Q., 2020. Nanoplastics display strong stability in aqueous environments: insights from aggregation behaviour and theoretical calculations. Environ. Pollut. 258, 113760 https://doi.org/10.1016/J.ENVPOL.2019.113760.

Massos, A., Turner, A., 2017. Cadmium, lead and bromine in beached microplastics. Environ. Pollut. 227, 139–145. https://doi.org/10.1016/J.ENVPOL.2017.04.034.

Mattsson, K., Johnson, E.V., Malmendal, A., Linse, S., Hansson, L.A., Cedervall, T., 2017. Brain damage and behavioural disorders in fish induced by plastic nanoparticles delivered through the food chain. Sci. Reports 7, 1–7. https://doi.org/10.1038/s41598-017-10813-0.

Pikuda, O., Xu, E.G., Berk, D., Tufenkji, N., 2019. Toxicity assessments of micro- and nanoplastics can be confounded by preservatives in commercial formulations. Environ. Sci. Technol. Lett. 6, 21–25. https://doi.org/10.1021/acs.estlett.8b00614.

Plastic production worldwide, 2021. Statista. https://www.statista.com/statistics/282732/global-production-of-plastics-since-1950/ (accessed May 25, 2024).

Ramirez, L., Gentile, S.R., Zimmermann, S., Stoll, S., 2019. Behavior of TiO2 and CeO2 nanoparticles and polystyrene nanoplastics in bottled mineral, drinking and Lake Geneva waters. Impact of water hardness and natural organic matter on nanoparticle surface properties and aggregation. Water 11, 721. https://doi.org/10.3390/W11040721.

Rodrigues, M.O., Abrantes, N., Gonçalves, F.J.M., Nogueira, H., Marques, J.C., Gonçalves, A.M.M., 2018. Spatial and temporal distribution of microplastics in water and sediments of a freshwater system (Antuã River, Portugal). Sci. Total Environ. 633, 1549–1559. https://doi.org/10.1016/J.SCITOTENV.2018.03.233.

Sharma, V.K., Ma, X., Guo, B., Zhang, K., 2021. Environmental factors-mediated behavior of microplastics and nanoplastics in water: a review. Chemosphere 271, 129597. https://doi.org/10.1016/J.CHEMOSPHERE.2021.129597.

Shi, Q., Tang, J., Liu, X., Liu, R., 2021. Ultraviolet-induced photodegradation elevated the toxicity of polystyrene nanoplastics on human lung epithelial A549 cells. Environ. Sci. Nano 8, 2660–2675. https://doi.org/10.1039/D1EN00465D.

Singh, N., Tiwari, E., Khandelwal, N., Darbha, G.K., 2019. Understanding the stability of nanoplastics in aqueous environments: effect of ionic strength, temperature, dissolved organic matter, clay, and heavy metals. Environ. Sci. Nano 6, 2968–2976. https://doi.org/10.1039/C9EN00557A.

Song, Y.K., Hong, S.H., Jang, M., Han, G.M., Jung, S.W., Shim, W.J., 2017. Combined effects of UV exposure duration and mechanical abrasion on microplastic fragmentation by polymer type. Environ. Sci. Technol. 51, 4368–4376. https://doi.org/10.1021/acs.est.6b06155.

Song, Y.K., Hong, S.H., Eo, S., Han, G.M., Shim, W.J., 2020. Rapid production of micro- and nanoplastics by fragmentation of expanded polystyrene exposed to sunlight. Environ. Sci. Technol. 54, 11191–11200. https://doi.org/10.1021/acs.est.0c02288.

Ter Halle, A., Jeanneau, L., Martignac, M., Jardé, E., Pedrono, B., Brach, L., Gigault, J., 2017. Nanoplastic in the North Atlantic subtropical gyre. Environ. Sci. Technol. 51, 13689–13697. https://doi.org/10.1021/acs.est.7b03667.

Tong, H., Zhong, X., Duan, Z., Yi, X., Cheng, F., Xu, W., Yang, X., 2022. Micro- and nanoplastics released from biodegradable and conventional plastics during degradation: formation, aging factors, and toxicity. Sci. Total Environ. 833, 155275 https://doi.org/10.1016/J.SCITOTENV.2022.155275.

Wang, Y., Li, P., Tran, T.T.D., Zhang, J., Kong, L., 2016. Manufacturing techniques and surface engineering of polymer based nanoparticles for targeted drug delivery to cancer. Nanomaterials 6, 26. https://doi.org/10.3390/NANO6020026.

Wang, X., Zheng, H., Zhao, J., Luo, X., Wang, Z., Xing, B., 2020. Photodegradation elevated the toxicity of polystyrene microplastics to grouper (Epinephelus Moara) through disrupting hepatic lipid homeostasis. Environ. Sci. Technol. 54, 6202–6212. https://doi.org/10.1021/acs.est.9b07016.

Wu, J., Jiang, R., Lin, W., Ouyang, G., 2019. Effect of salinity and humic acid on the aggregation and toxicity of polystyrene nanoplastics with different functional groups and charges. Environ. Pollut. 245, 836–843. https://doi.org/10.1016/J.ENVPOL.2018.11.055.

Wu, X., Liu, P., Zhao, X., Wang, J., Teng, M., Gao, S., 2022. Critical effect of biodegradation on long-term microplastic weathering in sediment environments: a systematic review. J. Hazard. Mater. 437, 129287 https://doi.org/10.1016/J.JHAZMAT.2022.129287.

Wu, X., Zhao, X., Chen, R., Liu, P., Liang, W., Wang, J., Shi, D., Teng, M., Wang, X., Gao, S., 2023. Size-dependent long-term weathering converting floating polypropylene macro- and microplastics into nanoplastics in coastal seawater environments. Water Res. 242, 120165 https://doi.org/10.1016/J.WATRES.2023.120165.

Zhang, B., Chao, J., Chen, L., Liu, L., Yang, X., Wang, Q., 2021. Research progress of nanoplastics in freshwater. Sci. Total Environ. 757, 143791 https://doi.org/10.1016/J.SCITOTENV.2020.143791.

Zielinska, A., Carreiró, F., Oliveira, A.M., Neves, A., Pires, B., Nagasamy Venkatesh, D., Durazzo, A., Lucarini, M., Eder, P., Silva, A.M., Santini, A., Souto, E.B., 2020. Polymeric nanoparticles: production, characterization, toxicology and ecotoxicology. Molecules 25, 3731. https://doi.org/10.3390/MOLECULES25163731.